Journal of Medicinal Chemistry

Article

pubs.acs.org/jmc

A Zinc(II) Phthalocyanine Conjugated with an Oxaliplatin Derivative for Dual Chemo- and Photodynamic Therapy

Janet T. F. Lau,[†] Pui-Chi Lo,*[,†] Wing-Ping Fong,[‡] and Dennis K. P. Ng*[,†]

[†]Department of Chemistry and [‡]School of Life Sciences, The Chinese University of Hong Kong, Shatin, N.T., Hong Kong, China

Supporting Information

ABSTRACT: A novel zinc(II) phthalocyanine substituted with an oxaliplatin derivative via a triethylene glycol linker has been synthesized. The two components work in a cooperative manner in the antitumor action. The conjugate shows a cytotoxic effect in the dark due to the cytostatic oxaliplatin moiety and an enhanced cytotoxicity upon illumination due to the photosensitizing phthalocyanine unit against the HT29 human colon adenocarcinoma cells. The IC_{50} value of the conjugate is as low as 0.11 μM, which is 5-fold lower than that of the reference compound without the platinum complex. The high photodynamic activity of the conjugate can be attributed to its high cellular uptake and efficiency in generating intracellular reactive oxygen species. The conjugate also shows preferential localization in the lysosomes of the cells and induces cell death mainly through apoptosis.

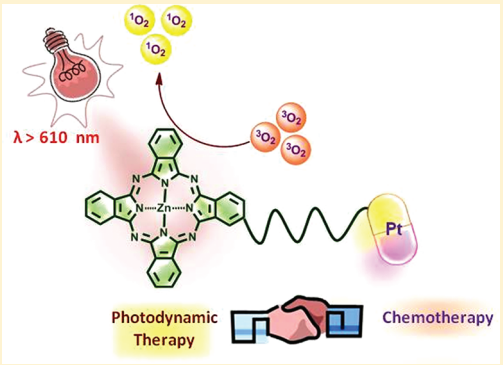

INTRODUCTION

Photodynamic therapy (PDT) is a clinically established treatment modality for a range of cancers and wet age-related macular degeneration.[1−3] It utilizes the combined action of a photosensitizer, light, and molecular oxygen to generate reactive oxygen species (ROS), particularly singlet oxygen, to eradicate cancer cells. The ROS generated through the photosensitization process react rapidly with biological substrates, triggering an apoptotic or necrotic response and eventually leading to oxidative damage of the cells.[4] Recently, there has been considerable interest in combining this modality with other anticancer therapeutic methods. The combination of modalities that act on different disease pathways has shown several advantages, such as enhanced therapeutic efficacy, reduced side effects, and retarded drug-resistance problem.[5] For dual PDT and chemotherapy, there are generally three approaches, including sequential administration of a photosensitizer and an anticancer drug, the use of their covalent and noncovalent conjugates, and coencapsulation of these agents in a polymeric nanocarrier. A number of anticancer drugs, including cisplatin,[6,7] carboplatin,[8,9] and doxorubicin,[10,11] have been evaluated for their outcomes in sequential treatment with PDT. For most of the cases, additive or synergistic effects have been observed which can reduce the effective doses of anticancer drugs. The sequence of the two treatment modalities has also been found to be crucial.[9,11,12]

A number of covalent conjugates of photosensitizers and platinum complexes have been prepared with a view to combining their cytotoxic effects.[13−18] Brunner et al. synthesized a series of these conjugates, which contain a porphyrin-based photosensitizing unit and a cisplatin derivative, and studied their antiproliferative activity toward several types of cancer cells.[13−15] The porphyrin moieties could generally enhance the cellular uptake and increase the antitumor activity of the platinum complexes. Guo et al. prepared another two conjugates in which a silicon(IV) phthalocyanine core is axially substituted with two cisplatin derivatives via the 3- or 4-pyridyloxy group.[16] These compounds were also photocytotoxic and potentially useful for DNA-targeting PDT. Recently, Donzello et al. have reported a series of tetra-2,3-pyrazinoporphyrazines appended with pyridine rings which can complex with a $PtCl_2$ moiety. The singlet oxygen generation efficiency of these conjugates and the interactions of one of these complexes with a telomeric DNA sequence having a G-quadruplex structure have also been studied.[17,18] Apart from these covalent conjugates, several noncovalent systems in which the photosensitizer and the anticancer drug are held either by host−guest interactions[19] or in polymeric nanocarriers[20−22] have also been prepared and briefly evaluated for their potential in dual PDT and chemotherapy.

Over the past decade, we have been interested in the development of efficient and selective photosensitizers for PDT. A vast number of novel photosensitizers based on phthalocyanines[23−25] and distyryl boron dipyrromethenes[26,27] have been synthesized and evaluated for their in vitro and in vivo photodynamic activities. In light of the potential advantages of combined chemo- and photodynamic therapy, we have recently extended our study to phthalocyanines substituted with platinum-based anticancer drugs. The latter have been widely used for the treatment of a variety of cancers through disruption of DNA in the nucleus.[28,29] It is believed that the combination of these two components can embrace the advantages of the two very different therapeutic mechanisms

Received: March 22, 2012
Published: May 31, 2012

dx.doi.org/10.1021/jm300398q | J. Med. Chem. 2012, 55, 5446−5454

Scheme 1. Synthesis of Phthalocyanine–Platinum Complex Conjugate 1

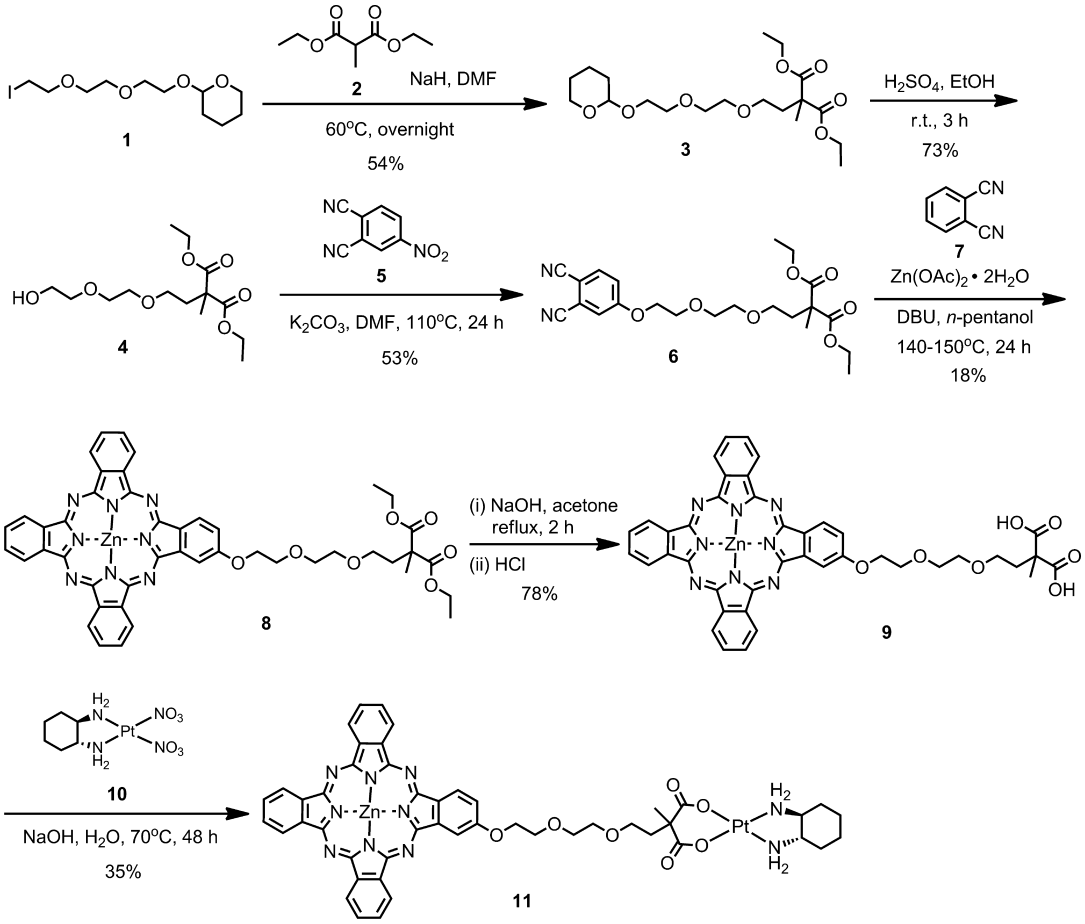

and the resulting conjugates can exhibit synergistic anticancer effects. In this paper, we report the preparation and in vitro photodynamic activities of such a conjugate, in which an oxaliplatin derivative is linked to a zinc(II) phthalocyanine core through a triethylene glycol spacer. The conjugate is highly potent of which the cytotoxicity is 5-fold higher than that of the analogue without the platinum complex, demonstrating the cooperative effects of the two cytotoxic components.

RESULTS AND DISCUSSION

Molecular Design and Synthesis. In this conjugate, a zinc(II) phthalocyanine was employed as the photosensitizing unit due to its near-infrared fluorescence emission, high singlet oxygen generation efficiency, and high photostability.[30−32] Owing to the high therapeutic efficacy of oxaliplatin,[28,29,33] a derivative of this drug was selected as the cytostatic part. The two components were linked with a triethylene glycol chain, which can enhance the amphiphilicity and biocompatibility of the system. Scheme 1 shows the synthetic route used to prepare this conjugate. Treatment of 1-iodo-8-(tetrahydro-2*H*-pyran-2-yloxy)-3,6-dioxaoctane (**1**)[34] with diethyl methylmalonate (**2**) and NaH in *N*,*N*-dimethylformamide (DMF) led to substitution giving compound **3**. The tetrahydropyranyl protecting group of **3** was then removed with concentrated sulfuric acid to give compound **4**. Nucleophilic aromatic substitution reaction of 4-nitrophthalonitrile (**5**) with alcohol **4** afforded the substituted phthalonitrile **6**. This compound then underwent mixed cyclization with an excess of phthalonitrile (**7**) in the presence of $Zn(OAc)_2{\cdot}2H_2O$ and 1,8-diazabicyclo[5.4.0]undec-7-ene (DBU) in *n*-pentanol to give the "3 + 1" unsymmetrical phthalocyanine **8** in 18% yield. This compound was then hydrolyzed with NaOH in acetone. After acidic treatment, the carboxyl derivative **9** was obtained, which was further complexed with *trans*-(1*R*,2*R*)-1,2-diaminocyclohexanedinitrato platinum(II) (**10**)[35] in an aqueous NaOH solution to give the phthalocyanine–platinum complex conjugate **11**. This compound was purified by flash column chromatography followed by recrystallization from a mixture of DMF and ethanol. For comparison, phthalocyanine **12** and oxaliplatin analogue **13** (Figure 1) were also prepared. The former was synthesized by

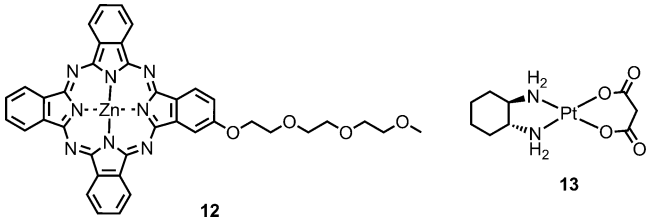

Figure 1. Structures of phthalocyanine **12** and oxaliplatin analogue **13**.

typical base-promoted mixed cyclization of 4-(3,6,9-trioxadecyloxy)phthalonitrile[36] with an excess of **7** in the presence of $Zn(OAc)_2{\cdot}2H_2O$, while the latter was prepared by treating **10** with an aqueous solution of malonic acid and KOH.[35] All the new compounds were fully characterized with various spectroscopic methods and elemental analysis (for

dx.doi.org/10.1021/jm300398q | J. Med. Chem. 2012, 55, 5446−5454

phthalocyanines **9**, **11**, and **12**) or accurate mass measurements (for phthalocyanine **8** and all the precursors).

Electronic Absorption and Photophysical Properties. The absorption spectrum of **11** in DMF was typical as the spectra of nonaggregated phthalocyanines (Figure S1 in the Supporting Information). It showed a B-band at 344 nm, two vibronic bands at 607 and 639 nm, and an intense and sharp Q-band at 672 nm, which strictly followed the Lambert−Beer's law. Upon excitation at 610 nm, the compound showed a fluorescence emission at 688 nm with a fluorescence quantum yield (Φ_F) of 0.22 relative to the unsubstituted zinc(II) phthalocyanine (ZnPc) (Φ_F = 0.28).[37] The spectral data of the reference compound **12** were very similar to those of **11**, except its slightly higher value of Φ_F (0.25), probably due to the absence of the heavy platinum complex (Figure S2 and Table S1 in the Supporting Information).

To evaluate the photosensitizing efficiency of these two compounds, their singlet oxygen quantum yields (Φ_Δ) were determined in DMF by a steady-state method with 1,3-diphenylisobenzofuran (DPBF) as the scavenger. The concentration of the quencher was monitored spectroscopically at 411 nm with time of irradiation (Figure S3 in the Supporting Information), from which the values of Φ_Δ could be determined by the method described previously.[38] The results showed that both compounds are highly efficient singlet oxygen generators, and the values of Φ_Δ were virtually identical to that of ZnPc (Φ_Δ = 0.56) (Table S1 in the Supporting Information).

In Vitro Photodynamic Activities. The cytotoxic effects of conjugate **11** in a Cremophor EL emulsion were then investigated. The surfactant was added to solubilize the compound in water and reduce its aggregation. Because oxaliplatin is one of the most important chemotherapeutic drugs in colorectal cancer treatment,[33] HT29 human colon adenocarcinoma cells were used for these studies. To reveal the photo- and chemocytotoxic effects of **11**, the antiproliferative properties of the two reference compounds **12** and **13** were also examined. Figure 2 shows the dose-dependent survival curves for these compounds. It can be seen in Figure 2a that the nonplatinum-containing phthalocyanine **12** does not show any dark toxicity up to 100 μM. However, upon illuminating with red light generated from a halogen lamp after passing through a color glass filter cut-on 610 nm, it shows substantial cytotoxicity with an IC_{50} value, defined as the dye concentration required to kill 50% of the cells, of 0.55 μM (Figure 2b, Table 1). The oxaliplatin analogue **13** exhibits cytostatic activity both in the absence and presence of light, and the corresponding IC_{50} values are 10.7 and 5.5 μM, respectively. It is interesting to note the enhanced cytotoxicity under illumination, although the actual mechanism remains elusive at this stage. Having a photosensitizer and a chemotherapeutic drug in the same molecule, conjugate **11** is highly photocytotoxic. The IC_{50} value is as low as 0.11 μM, which is 5-fold lower than that of **12**. In fact, this conjugate is much more potent than the classical photosensitizer porfimer sodium, which has an IC_{50} value of 4.5 μg mL^{-1} under the same experimental conditions (vs 0.12 μg mL^{-1} for **11**). Its cytotoxicity is also significantly higher than that of oxaliplatin, of which the IC_{50} value was found to be ca. 0.9 μM.[39] Conjugate **11** also exhibits some dark toxicity (IC_{50} = 78.5 μM), which can be attributed to the oxaliplatin moiety as **12** is nontoxic under these conditions. As a better control, the cytotoxicity of an equimolar mixture of **12** and **13** was also studied and compared with that of **11**. It can be seen in Figure 2b and Table 1 that the mixture is relatively more potent than **12** alone (IC_{50} = 0.42 vs 0.55 μM), probably due to the additional antitumor effect of the oxaliplatin derivative. However, its photocytotoxicity is still significantly lower than that of **11** (IC_{50} = 0.42 vs 0.11 μM). The results clearly show that the two antitumor components in conjugate **11** work in a cooperative fashion.

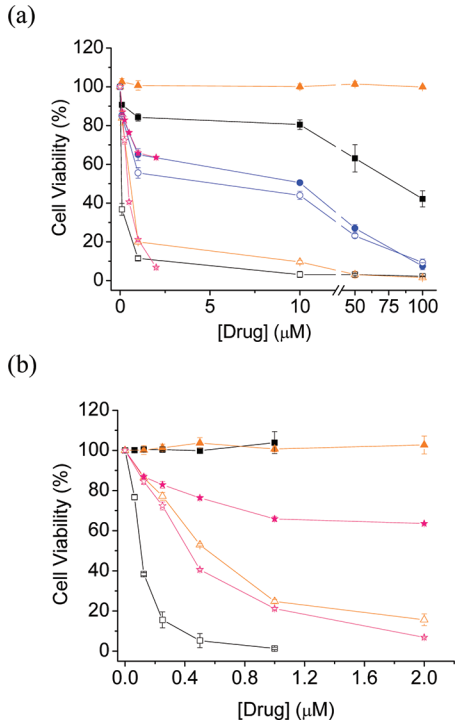

Figure 2. (a) Comparison of the cytotoxic effects of **11** (squares), **12** (triangles), **13** (circles), and an equimolar mixture of **12** and **13** (stars) on HT29 cells in the absence (closed symbols) and presence (open symbols) of light (λ > 610 nm, 40 mW cm^{-2}, 48 J cm^{-2}). Data are expressed as mean value ± standard error of the mean value (SEM) of three independent experiments, each performed in quadruplicate. (b) Data for **11** (squares), **12** (triangles), and an equimolar mixture of **12** and **13** (stars) in the range up to 2.0 μM.

Table 1. IC_{50} Values for 11−13 and an Equimolar Mixture of 12 and 13 against HT29 Cells

compd	IC_{50} (μM)	
	in dark	with light
11	78.5	0.11
12	*a*	0.55
13	10.7	5.5
1:1 mixture of **12** and **13**	*b*	0.42

[a]Noncytotoxic up to 100 μM. [b]Not determined.

Considering the fact that the aggregation state of photosensitizers is an important factor relating to their photodynamic activities,[30−32] the aggregation behavior of conjugate **11** and the reference compound **12**, formulated with Cremophor EL in Dulbecco's Modified Eagle's Medium (DMEM), was examined by absorption and fluorescence spectroscopic methods. As shown in Figure S4 in the Supporting Information, both compounds show a relatively sharp and intense Q-band and a relatively strong fluorescence emission. The results suggest that both compounds are not significantly aggregated under these

dx.doi.org/10.1021/jm300398q | J. Med. Chem. 2012, 55, 5446−5454

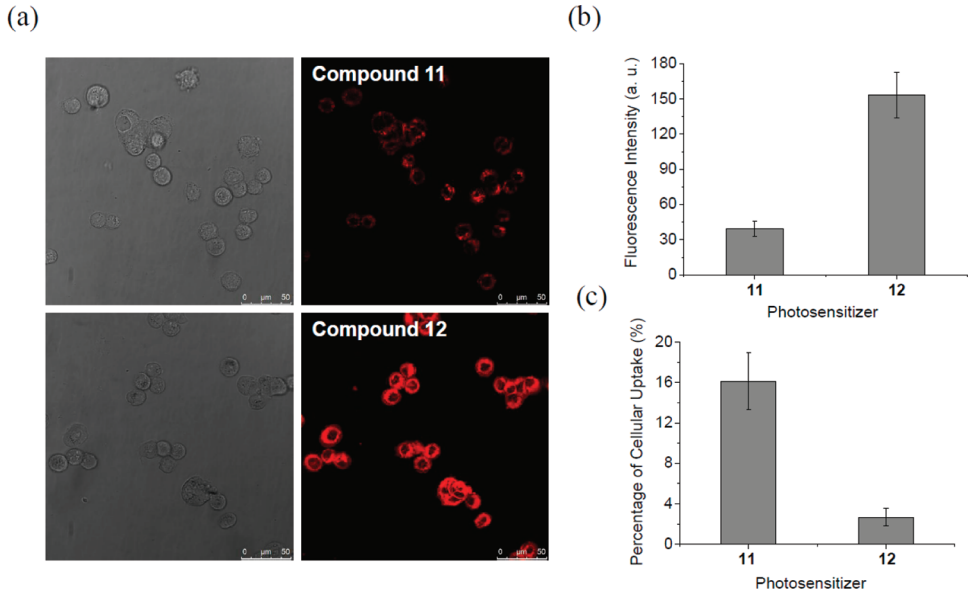

Figure 3. (a) Confocal fluorescence images of HT29 cells after incubation with **11** or **12** for 2 h (both at 5 μM). The corresponding bright field images are given in the left column. (b) Comparison of the relative intracellular fluorescence intensity of **11** and **12** (number of cells = 30). (c) Comparison of the percentage of cellular uptake of **11** and **12** as determined by an extraction method. Data are expressed as mean value ± standard deviation (SD) of three independent experiments.

conditions, which seems to be in accord with their high photocytotoxicity.

To account for the different photocytotoxicity of these two compounds, their cellular uptake was examined by fluorescence microscopy and absorption spectroscopy. As shown by the images captured by confocal laser scanning microscopy (Figure 3a), both compounds could enter into the cells causing intracellular fluorescence after incubation for 2 h. The average relative fluorescence intensity per cell of these compounds was also measured and compared in Figure 3b. It can be seen that the intracellular fluorescence intensity of **11** is about 5-fold lower than that of **12**. However, to take into account that these two compounds may have different efficiency in generating fluorescence inside the cells, an extraction method was also employed to quantify the cellular uptake. After incubation with these phthalocyanines, DMF was used to lyse the cells and extract the dyes. The dye concentrations inside the cells were quantified by measuring their Q-band absorbance at 672 nm. The results are depicted in Figure 3c, which shows that the cellular uptake of **11** is actually about 7-fold higher than that of **12**. The presence of the oxaliplatin derivative in **11** may enhance the amphiphilicity of the overall compound, thereby promoting the cellular uptake. The higher cellular uptake of **11** is in accord with its higher photocytotoxicity.

In addition, the intracellular production of ROS by these compounds was also studied using 2′,7′-dichlorodihydrofluorescein diacetate (DCFDA) as the quencher.[40] As shown in Figure 4, both **11** and **12** as well as the mixture of **12** and **13** can sensitize the production of ROS upon illumination. Conjugate **11** is the most efficient compound in producing intracellular ROS, which may be a result of its higher cellular uptake. Because the oxaliplatin derivative **13** is not a photosensitizer, it is expected that it does not produce any ROS even after illumination. The ROS production efficiencies of **12** and the mixture of **12** and **13** are therefore comparable to each other. All these results suggest that the higher photocytotoxicity of conjugate **11** can be attributed to its low

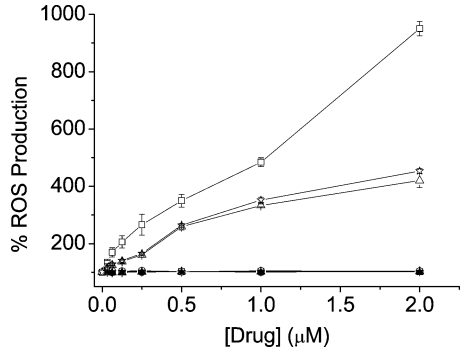

Figure 4. ROS production induced by **11** (squares), **12** (triangles), **13** (circles), and an equimolar mixture of **12** and **13** (stars) in HT29 cells in the absence (closed symbols) and presence (open symbols) of light (λ > 610 nm, 40 mW cm^{-2}, 48 J cm^{-2}). Data are expressed as mean value ± SEM of three independent experiments, each performed in quadruplicate.

aggregation tendency and higher cellular uptake and efficiency in generating intracellular ROS.

The subcellular localization of conjugate **11** was also investigated. The cells were first incubated with the compound in the culture medium for 2 h, and then stained with LysoTracker DND 26, ER-Tracker Green, MitoTracker Green FM, or SYTO-16 (for 10−20 min), which are specific dyes for lysosomes, endoplasmic reticulum, mitochondria, and nucleus, respectively. As shown in Figure 5, the fluorescence caused by the LysoTracker (excited at 488 nm, monitored at 510−570 nm) can superimpose with the fluorescence caused by **11** (excited at 633 nm, monitored at 650−750 nm). The very similar fluorescence intensity line profiles of **11** and LysoTracker traced along the green line in Figure 5a (iv) also confirms that **11** can target the lysosomes of the cells. By contrast, the fluorescence images of **11** could not be merged with those of the ER-Tracker, MitoTracker, and SYTO-16 (excited at 488 nm, monitored at 510−570 nm) (Figure S5 in

dx.doi.org/10.1021/jm300398q | J. Med. Chem. 2012, 55, 5446−5454

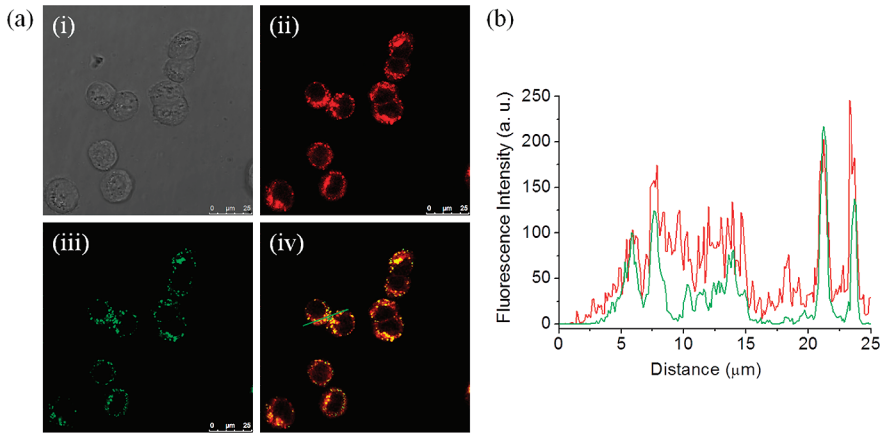

Figure 5. (a) Visualization of (i) the bright field image, intracellular fluorescence of HT29 using filter sets specific for (ii) **11** (in red) and (iii) LysoTracker (in green), and (iv) the corresponding superimposed image. (b) Fluorescence intensity profiles of **11** (red) and LysoTracker (green) traced along the green line in (a) (iv).

the Supporting Information), showing that **11** is not localized in the endoplasmic reticulum, mitochondria, and nucleus of the cells.

To determine the mode of cell death induced by **11**, a flow cytometric assay of annexin V-green fluorescent protein (GFP) and propidium iodide (PI) double staining was employed.[41] To find out whether the introduction of the oxaliplatin derivative will alter the cell death mechanism, the results for **12** and **13** were also compared. The cell populations in different phases of cell death, namely viable (annexin V-GFP$^-$/PI$^-$), early apoptotic (annexin V-GFP$^+$/PI$^-$), and necrotic or late-stage apoptotic (annexin V-GFP$^+$/PI$^+$) were examined at the respective IC_{50} values of the drugs. The only exception was for **12** in the dark for which the IC_{50} value could not be determined, a dye concentration of 100 μM was used for the measurements. As shown in Table 2, when the cells were treated with **11** or **12** in the presence of light, about 50% of apoptotic cells and less than 10% of necrotic cells were observed. Compound **11** also exhibited a significant dark toxicity, showing 41% of apoptotic cells and 9% of necrotic cells after the treatment due to the oxaliplatin derivative. For **12** in the dark, more than 95% of the tumor cells remained viable even at 100 μM. The oxaliplatin derivative **13** could induce apoptotic as well as necrotic cells, both in the absence and presence of light. The results showed that apoptosis is the major pathway for the PDT action of **11** and the presence of the oxaliplatin derivative does not significantly affect the cell death pathways.

Table 2. Flow Cytometric Analysis of the Cell Death Mechanism Induced by 11, 12, and 13 at Their Respective IC_{50} Values in the Absence and Presence of Light on HT29 Cells[a]

			cell population (%)		
	[Drug] (μM)	illumination	viable	apoptotic	necrotic
blank	0	−	95.0 ± 1.2	3.3 ± 0.5	1.2 ± 0.3
11	0.11	+	36.5 ± 1.1	54.2 ± 2.9	8.4 ± 1.6
	78	−	48.9 ± 1.5	41.0 ± 1.2	9.3 ± 0.7
12	0.55	+	44.9 ± 1.9	50.2 ± 1.9	4.4 ± 0.7
	100[b]	−	95.3 ± 1.8	2.2 ± 1.5	2.1 ± 1.2
13	5.5	+	45.2 ± 4.8	41.4 ± 1.8	13.0 ± 3.1
	10.7	−	53.8 ± 3.5	25.7 ± 3.0	19.9 ± 0.6

[a]Data are expressed as mean value ± SD of three independent experiments. [b]The IC_{50} value could not be determined.

CONCLUSIONS

In summary, we have synthesized and characterized a zinc(II) phthalocyanine−platinum complex conjugate and evaluated its in vitro photodynamic activities. This conjugate contains both photo- and chemotherapeutic agents which are covalently linked and function in a cooperative manner. The introduction of the oxaliplatin derivative can enhance the cellular uptake and intracellular ROS generation efficiency of the phthalocyanine unit, resulting in a higher cytotoxicity. The IC_{50} value of the conjugate is as low as 0.11 μM toward the HT29 cells, which is 5-fold lower than that of the reference compound without the oxaliplatin derivative. The conjugate also shows preferential localization in the lysosomes of the cells and induces cell death mainly through apoptosis. The overall results show that this conjugate is a highly promising antitumor agent for dual chemo- and photodynamic therapy.

EXPERIMENTAL SECTION

General. All the reactions were performed under an atmosphere of nitrogen. DMF was predried with barium oxide and distilled under reduced pressure. *n*-Pentanol was distilled from sodium under reduced pressure. Chromatographic purifications were performed on silica gel (Macherey−Nagel, 230−400 mesh) columns with the indicated eluents. Size exclusion chromatography was carried out on Bio-Rad Bio-Beads S-X1 beads (200−400 mesh) with THF as the eluent. All other solvents and reagents were of reagent grade and used as received. Compounds **1**,[34] **10**,[35] and **13**[35] were prepared as described.

^{1}H and ^{13}C{^{1}H} NMR spectra were recorded on a Bruker AVANCE III 400 spectrometer (^{1}H, 400; ^{13}C, 100.6 MHz) in $CDCl_3$ unless otherwise stated. Spectra were referenced internally using the residual solvent (^{1}H: δ 7.26) or solvent (^{13}C: δ 77.2) resonances relative to $SiMe_4$. Electrospray ionization (ESI) mass spectra were recorded on a Thermo Finnigan MAT 95 XL mass spectrometer. Elemental analyses were performed by the Shanghai Institute of Organic Chemistry, Chinese Academy of Sciences, China. The purity of all the new compounds was determined by elemental analysis (for **9**, **11**, and **12**) or ^{1}H NMR spectroscopy and was found to be ≥95%.

dx.doi.org/10.1021/jm300398q | J. Med. Chem. 2012, 55, 5446−5454

UV−vis and steady-state fluorescence spectra were taken on a Cary 5G UV−vis−NIR spectrophotometer and a Hitachi F-7000 spectrofluorometer, respectively. The fluorescence quantum yields of the samples [$\Phi_{F(sample)}$] were determined by the equation: $\Phi_{F(sample)} = (F_{sample}/F_{ref})(A_{ref}/A_{sample})(n_{sample}^2/n_{ref}^2)\Phi_{F(ref)}$,[42] where F, A, and n are the measured fluorescence (area under the emission peak), the absorbance at the excitation position, and the refractive index of the solvent, respectively. ZnPc in DMF was used as the reference [$\Phi_{F(ref)} = 0.28$].[37]

Compound 3. Diethyl methylmalonate (**2**) (4.00 g, 22.96 mmol) was added to a slurry suspension of NaH (0.83 g, 34.58 mmol) in DMF (30 mL) at 0 °C under a nitrogen atmosphere. A solution of **1** (7.90 g, 22.95 mmol) in DMF (30 mL) was then added in dropwise to the reaction mixture. The mixture was heated at 60 °C for 24 h, and then the solvent was evaporated under reduced pressure. The residue was then subject to silica gel column chromatography using ethyl acetate/hexane (9:1 v/v) as the eluent to obtain the product as a yellow oily liquid (4.83 g, 54%). R_f [ethyl acetate/hexane (9:1 v/v)] = 0.42. ^{1}H NMR: δ = 4.62 (t, J = 4.0 Hz, 1 H, CH), 4.16 (dq, J = 2.0, 7.2 Hz, 4 H, CH_2), 3.83−3.89 (m, 2 H, CH_2), 3.47−3.67 (m, 10 H, CH_2), 2.18 (t, J = 6.4 Hz, 2 H, CH_2), 1.67−1.87 (m, 3 H, CH and CH_2), 1.48−1.63 (m, 3 H, CH and CH_2), 1.43 (s, 3 H, CH_3), 1.24 (t, J = 7.2 Hz, 6 H, CH_3). ^{13}C{^{1}H} NMR: δ = 172.1, 98.9, 70.5 (two overlapping signals), 70.2, 67.2, 66.6, 62.2, 61.2, 52.0, 35.0, 30.5, 25.4, 20.0, 19.5, 14.0. MS (ESI): m/z 413 (100%, [M + Na]$^+$). HRMS (ESI): m/z calcd for $C_{19}H_{34}NaO_8$ [M + Na]$^+$, 413.2146; found, 413.2145.

Compound 4. Concentrated sulfuric acid (5 drops) was added to a solution of **3** (1.08 g, 2.77 mmol) in ethanol (10 mL). The mixture was stirred at room temperature for 3 h, and then it was neutralized with an aqueous solution of $NaHCO_3$. The solvent was evaporated under reduced pressure, and then the residue was redissolved in diethyl ether. The insoluble material was removed by filtration. The filtrate was evaporated to give a pale-yellow oil (0.62 g, 73%). ^{1}H NMR: δ = 4.16 (dq, J = 2.8, 7.2 Hz, 4 H, CH_2), 3.72 (t, J = 4.0 Hz, 2 H, CH_2), 3.52−3.61 (m, 8 H, CH_2), 2.19 (t, J = 6.4 Hz, 2 H, CH_2), 1.43 (s, 3 H, CH_3), 1.23 (t, J = 7.2 Hz, 6 H, CH_3). ^{13}C{^{1}H} NMR: δ = 172.2, 72.4, 70.3, 70.2, 67.1, 61.8, 61.3, 51.9, 35.0, 19.9, 14.0. MS (ESI): m/z 329 (100%, [M + Na]$^+$). HRMS (ESI): m/z calcd for $C_{14}H_{26}NaO_7$ [M + Na]$^+$, 329.1571; found, 329.1580.

Phthalonitrile 6. A mixture of **4** (0.58 g, 1.89 mmol), 4-nitrophthalonitrile (**5**) (0.16 g, 0.92 mmol), and K_2CO_3 (0.38 g, 2.75 mmol) in DMF (20 mL) was stirred at 110 °C under nitrogen for 24 h. The solvent was removed at 60 °C under reduced pressure. The residue was mixed with H_2O (50 mL), and then it was extracted with $CHCl_3$ (50 mL × 3). The combined organic layers was dried over anhydrous Na_2SO_4, filtered, and concentrated in vacuo. The crude product was subject to silica gel column chromatography using hexane/ethyl acetate (1:1 v/v) as the eluent to afford the product as a pale-yellow oil (0.21 g, 53%). R_f [hexane/ethyl acetate (1:1 v/v)] = 0.29. ^{1}H NMR: δ = 7.70 (d, J = 8.8 Hz, 1 H, ArH), 7.31 (d, J = 2.8 Hz, 1 H, ArH), 7.23 (dd, J = 2.8, 8.8 Hz, 1 H, ArH), 4.22 (t, J = 4.8 Hz, 2 H, CH_2), 4.16 (dq, J = 2.4, 7.2 Hz, 4 H, CH_2), 3.85−3.89 (m, 2 H, CH_2), 3.64−3.69 (m, 2 H, CH_2), 3.47−3.59 (m, 4 H, CH_2), 2.18 (t, J = 6.4 Hz, 2 H), 1.42 (s, 3 H, CH_3), 1.23 (t, J = 7.2 Hz, 6 H, CH_3). ^{13}C{^{1}H} NMR: δ = 172.1, 162.0, 135.2, 119.8, 119.5, 117.4, 115.6, 115.2, 107.4, 70.9, 70.2, 69.1, 68.6, 67.3, 61.2, 51.9, 35.0, 20.0, 14.0. MS (ESI): m/z 455 (100%, [M + Na]$^+$). HRMS (ESI): m/z calcd for $C_{22}H_{28}N_2NaO_7$ [M + Na]$^+$, 455.1789; found, 455.1800.

Phthalocyanine 8. A mixture of **6** (0.53 g, 1.23 mmol), phthalonitrile (**7**) (1.42 g, 11.08 mmol), and $Zn(OAc)_2{\cdot}2H_2O$ (0.81 g, 3.69 mmol) in n-pentanol (25 mL) was heated to 100 °C, and then a small amount of DBU (1 mL) was added. The mixture was stirred at 140−150 °C for 24 h. After cooling, the volatiles were removed under reduced pressure. The residue was dissolved in $CHCl_3$ (150 mL), and then part of the ZnPc formed was removed by filtration. The filtrate was collected and evaporated to dryness in vacuo. The residue was purified by silica gel column chromatography using $CHCl_3$ and then $CHCl_3$/MeOH (100:1 v/v) as the eluents. The crude product was purified by size exclusion chromatography with Bio-Beads S-X1 beads using THF as the eluent. The product was then further purified by recrystallization from a mixture of THF and hexane to give a green solid (0.19 g, 18%). ^{1}H NMR ($CDCl_3$ with a trace amount of pyridine-d_5): δ = 8.92−9.10 (m, 6 H, Pc-H$_\alpha$), 8.71 (d, J = 8.0 Hz, 1 H, Pc-H$_\alpha$), 8.24 (s, 1 H, Pc-H$_\alpha$), 7.89−8.01 (m, 6 H, Pc-H$_\beta$), 7.42 (d, J = 8.0 Hz, 1 H, Pc-H$_\beta$), 4.57 (virtual t, J = 4.4 Hz, 2 H, CH_2), 4.16−4.23 (m, 6 H, CH_2), 3.91 (t, J = 4.4 Hz, 2 H, CH_2), 3.74 (t, J = 4.4 Hz, 2 H, CH_2), 3.66 (t, J = 6.8 Hz, 2 H, CH_2), 2.30 (t, J = 6.8 Hz, 2 H, CH_2), 1.50 (s, 3 H, CH_3), 1.25 (t, J = 7.2 Hz, 6 H, CH_3). ^{13}C{^{1}H} NMR ($CDCl_3$ with a trace amount of pyridine-d_5): δ = 172.1, 160.1, 153.0, 152.9, 152.7, 152.6, 152.3, 152.2, 139.8, 138.1, 138.0, 137.9, 137.7, 131.2, 128.6, 128.5, 128.4, 128.3, 123.1, 122.2, 122.1, 122.0, 117.9, 104.8, 70.9, 70.4, 69.9, 67.9, 67.3, 61.2, 52.0, 35.1, 20.0, 14.0 (some of the aromatic signals were overlapped). MS (ESI): an isotopic cluster peaking at m/z 881 (80%, [M + H]$^+$). HRMS (ESI): m/z calcd for $C_{46}H_{41}N_8O_7Zn$ [M + H]$^+$, 881.2384; found, 881.2391.

Phthalocyanine 9. A mixture of **8** (0.15 g, 0.17 mmol), 5 M NaOH (0.3 mL, 1.5 mmol), and acetone (20 mL) was heated under reflux for 2 h. The volatiles were removed under reduced pressure. The green residue was washed thoroughly with acetone, and then redissolved in water and acidified with 3 M HCl until pH = 4. The green precipitate was washed thoroughly with water and ethanol, and then dried in vacuo (0.11 g, 78%). ^{1}H NMR (DMSO-d_6 with a trace amount of pyridine-d_5): δ = 9.25−9.34 (m, 6 H, Pc-H$_\alpha$), 9.05 (d, J = 8.0 Hz, 1 H, Pc-H$_\alpha$), 8.65 (d, J = 2.0 Hz, 1 H, Pc-H$_\alpha$), 8.17−8.23 (m, 6 H, Pc-H$_\beta$), 7.69 (dd, J = 2.0, 8.0 Hz, 1 H, Pc-H$_\beta$), 4.66 (virtual t, J = 4.4 Hz, 2 H, CH_2), 4.08 (virtual t, J = 4.4 Hz, 2 H, CH_2), 3.80 (t, J = 4.4 Hz, 2 H, CH_2), 3.64 (t, J = 4.4 Hz, 2 H, CH_2), 3.53 (t, J = 7.2 Hz, 2 H, CH_2), 2.08 (t, J = 7.2 Hz, 2 H, CH_2), 1.35 (s, 3 H, CH_3). ^{13}C{^{1}H} NMR (DMSO-d_6 with a trace amount of pyridine-d_5): δ = 174.3, 160.3, 152.8, 152.6, 152.4, 152.2, 152.1, 139.9, 138.0, 137.8, 137.7, 130.9, 129.2, 129.0, 123.2, 122.4, 122.2, 117.9, 105.4, 70.4, 70.0, 69.5, 68.1, 67.4, 51.2, 35.5, 20.9 (some of the aromatic signals were overlapped). MS (ESI): isotopic clusters peaking at m/z 780 (100%, [M − CO_2]$^+$) and 824 (35%, M$^+$). HRMS (ESI): m/z calcd for $C_{42}H_{32}N_8O_7Zn$ [M]$^+$, 824.1680; found, 824.1654. Anal. Calcd for $C_{42}H_{32}N_8O_7Zn$: C, 61.06; H, 3.90; N, 13.56. Found: C, 60.81; H, 3.56; N, 13.27.

Phthalocyanine 11. Phthalocyanine **9** (0.25 g, 0.30 mmol) was dissolved in water (50 mL) containing 5 M NaOH (0.15 mL, 0.75 mmol). It was then added to a solution of **10** (0.13 g, 0.30 mmol) in water (30 mL). The mixture was heated at 70 °C for 48 h. The resulting blue precipitate was filtered and washed thoroughly with water and ethanol. The crude product was then subject to flash silica gel column chromatography using DMF as the eluent. The product was further purified by recrystallization from a mixture of DMF and ethanol to afford a blue solid (0.12 g, 35%). R_f (DMF) = 0.65. ^{1}H NMR (DMSO-d_6 with a trace amount of pyridine-d_5): δ = 9.38−9.44 (m, 6 H, Pc-H$_\alpha$), 9.24 (d, J = 8.4 Hz, 1 H, Pc-H$_\alpha$), 8.87 (d, J = 2.0 Hz, 1 H, Pc-H$_\alpha$), 8.21−8.24 (m, 6 H, Pc-H$_\beta$), 7.77 (dd, J = 2.0, 8.4 Hz, 1 H, Pc-H$_\beta$), 4.67 (virtual t, J = 4.4 Hz, 2 H, CH_2), 4.04 (virtual t, J = 4.4 Hz, 2 H, CH_2), 3.75 (t, J = 4.4 Hz, 2 H, CH_2), 3.61 (t, J = 4.4 Hz, 2 H, CH_2), 3.53 (t, J = 7.2 Hz, 2 H, CH_2), 2.34 (br s, 2 H, CH_2), 1.88−1.97 (m, 4 H, CH_2), 1.49 (br s, 2 H, CH_2), 1.16−1.37 (m, 5 H, CH_2 and CH_3), 0.98−1.05 (m, 2 H, CH_2). The ^{13}C{^{1}H} NMR spectrum could not be obtained due to its low solubility in common organic solvents. MS (ESI): an isotopic cluster peaking at m/z 1133 (38%, [M + H]$^+$). HRMS (ESI): m/z calcd for $C_{48}H_{45}N_{10}O_7PtZn$ [M + H]$^+$, 1133.2404; found, 1133.2415. Anal. Calcd for $C_{48}H_{44}N_{10}O_7PtZn$: C, 50.87; H, 3.91; N, 12.35. Found: C, 50.50; H, 3.63; N, 11.95.

Phthalocyanine 12. A mixture of phthalocyanine (**7**) (2.06 g, 16.08 mmol), 4-(3,6,9-trioxadecyloxy)phthalonitrile[36] (0.52 g, 1.79 mmol), and $Zn(OAc)_2{\cdot}2H_2O$ (1.18 g, 5.38 mmol) in n-pentanol (20 mL) was heated to 100 °C, and then a small amount of DBU (1 mL) was added. The mixture was stirred at 140−150 °C for 24 h. After a brief cooling, the volatiles were removed under reduced pressure. The residue was dissolved in $CHCl_3$ (150 mL) and then filtered to remove part of the ZnPc formed. The filtrate was collected and evaporated to dryness in vacuo. The residue was purified by silica gel column chromatography using $CHCl_3$ and then $CHCl_3$/MeOH (100:1 v/v) as the eluents. The crude product was purified by size exclusion

chromatography using THF as the eluent followed by recrystallization from a mixture of $CHCl_3$ and hexane to give a green solid (0.32 g, 24%). ^{1}H NMR ($CDCl_3$ with a trace amount of pyridine-d_5): δ = 9.05−9.10 (m, 3 H, Pc-H$_\alpha$), 9.01 (d, J = 7.2 Hz, 1 H, Pc-H$_\alpha$), 8.95 (d, J = 6.4 Hz, 1 H, Pc-H$_\alpha$), 8.90 (d, J = 6.8 Hz, 1 H, Pc-H$_\alpha$), 8.68 (d, J = 8.0 Hz, 1 H, Pc-H$_\alpha$), 8.20 (d, J = 2.0 Hz, 1 H, Pc-H$_\alpha$), 7.88−8.01 (m, 6 H, Pc-H$_\beta$), 7.39 (dd, J = 2.0, 8.0 Hz, 1 H, Pc-H$_\beta$), 4.57 (virtual t, J = 4.4 Hz, 2 H, CH_2), 4.19 (virtual t, J = 4.4 Hz, 2 H, CH_2), 3.97−3.99 (m, 2 H, CH_2), 3.85−3.87 (m, 2 H, CH_2), 3.77−3.79 (m, 2 H, CH_2), 3.64−3.66 (m, 2 H, CH_2), 3.42 (s, 3 H, CH_3). ^{13}C{^{1}H} NMR ($CDCl_3$ with a trace amount of pyridine-d_5): δ = 160.2, 153.2, 152.9, 152.8, 152.5, 139.9, 138.1, 138.0, 137.8, 131.3, 128.7, 128.5, 123.2, 122.3, 118.1, 105.1, 71.9, 71.0, 70.8, 70.6, 70.0, 68.0, 59.0 (some of the aromatic signals were overlapped). MS (ESI): an isotopic cluster peaking at m/z 738 (100%, M$^+$). HRMS (ESI): m/z calcd for $C_{39}H_{30}N_8O_4Zn$ [M]$^+$, 738.1676; found, 738.1674. Anal. Calcd for $C_{39}H_{30}N_8O_4Zn$: C, 63.29; H, 4.09; N, 15.13. Found: C, 63.52; H, 4.35; N, 14.75.

Cell Lines and Culture Conditions. The HT29 human colon adenocarcinoma cells (from ATCC, no. HTB-38) were maintained in DMEM (Invitrogen, cat no. 10313−021) supplemented with fetal calf serum (10%), penicillin−streptomycin (100 units mL^{-1} and 100 μg mL^{-1} respectively), L-glutamine (2 mM), and transferrin (10 μg mL^{-1}).

Photocytotoxicity Assay. Approximately 3 × 10^4 HT29 cells per well in the culture medium were inoculated in 96-multiwell plates and incubated overnight at 37 °C in a humidified 5% CO_2 atmosphere. Compounds **11**−**13** were first dissolved in DMF to give 10 mM solutions, which were diluted to 1 mM with the culture medium in the presence of 0.5% Cremophor EL. These served as the stock solutions for the following in vitro studies. For cytotoxicity studies, the solutions were further diluted with the culture medium. The cells, after being rinsed with phosphate buffered saline (PBS), were incubated with 100 μL of the diluted phthalocyanine solutions for 2 h at 37 °C under 5% CO_2. The cells were then rinsed again with PBS and refed with 100 μL of the culture medium before being illuminated at ambient temperature. The light source consisted of a 300 W halogen lamp, a water tank for cooling, and a color glass filter (Newport) cut-on 610 nm. The fluence rate (λ > 610 nm) was 40 mW cm^{-2}. Illumination of 20 min led to a totally fluence of 48 J cm^{-2}.

Cell viability was determined by means of the colormetric MTT assay.[43] After illumination, the cells were incubated at 37 °C under 5% CO_2 overnight. An MTT (Sigma) solution in PBS (3 mg mL^{-1}, 50 μL) was added to each well followed by incubation for 2 h under the same environment. A solution of sodium dodecyl sulfate (SDS; Sigma, 10% by weight, 50 μL) was then added to each well. The plate was incubated in an oven at 60 °C for 30 min, and then 80 μL of isopropyl alcohol was added to each well. The plate was agitated on a Bio-Rad microplate reader at ambient temperature for 10 s before the absorbance at 540 nm at each well was taken. The average absorbance of the blank wells, which did not contain the cells, was subtracted from the readings of the other wells. The cell viability was then determined by the equation: % Viability = $[\sum(A_i/A_{control} \times 100)]/n$, where A_i is the absorbance of the ith data (i = 1, 2, ..., n), $A_{control}$ is the average absorbance of the control wells, in which the phthalocyanine was absent, and n (= 4) is the number of data points.

ROS Measurements. ROS production was determined by using DCFDA (Molecular Probes) as the quencher.[40] Approximately 3 × 10^4 HT29 cells per well in the culture medium was inoculated in a 96-multiwell plate for 24 h before photodynamic treatment. After the cells were incubated with different concentrations of the drugs in the medium (2-fold dilution from 2 μM, 100 μL) for 2 h in darkness, the cells were rinsed with PBS before 100 μL of DCFDA (10 μM in PBS) was added to each well. The mixture was incubated at 37 °C under 5% CO_2 for 30 min in darkness, followed by illumination for 20 min. Fluorescence measurements were made in a fluorescence plate reader (TECAN Polarion) with a 485 nm excitation filter and a 535 nm emission filter set at a gain of 60.

Cellular Uptake (Determined by Confocal Microscopy). About 6 × 10^4 HT29 cells in the culture medium (2 mL) were seeded on a coverslip and incubated overnight at 37 °C under 5% CO_2. The medium was removed, and then the cells were incubated with **11** or **12** in the medium (5 μM, 2 mL) for 2 h under the same conditions. The cells were then rinsed with PBS twice and viewed with a Leica SP5 confocal laser-scanning microscope equipped with a 633 nm helium−neon laser. The emission signals in 650−750 nm were collected, and the images were digitized and analyzed by Leica Application Suite Advanced Fluorescence Software. The intracellular fluorescence intensities (a total of 30 cells in each sample) were also determined.

Cellular Uptake (Determined by Extraction). About 2.0 × 10^6 HT29 cells in the culture medium (2 mL) were seeded on a Petri dish (diameter = 35 mm) and incubated overnight at 37 °C under 5% CO_2. The medium was removed, and the cells were rinsed with PBS (2 mL). The cells were then incubated with a solution of **11** or **12** in the medium (5 μM, 2 mL) for 2 h under the same conditions. The solution was then removed and the cells were rinsed with PBS (2 mL) and then harvested by 0.25% trypsin-EDTA (Invitrogen, 500 μL), followed by quenching the trypsin with medium (500 μL). The solution was transferred to 1.5 mL centrifuge tubes and centrifuged at 2400 rpm for 3 min. The pellet was then washed with PBS (1 mL), and the suspension was centrifuged again. After removing the PBS, the cells were lysed with DMF (1 mL). The mixture was sonicated for 20 min and then centrifuged again. The supernatants were transferred for UV−vis spectroscopic measurements. The absorbance at 672 nm for both phthalocyanines was compared with the respective calibration curves to give the uptake concentrations. Each experiment was repeated three times.

Subcellular Localization Studies. About 3 × 10^4 HT29 cells in the culture medium (2 mL) were seeded on a coverslip and incubated overnight at 37 °C under 5% CO_2. The medium was then removed. The cells were incubated with a solution of **11** in the medium (5 μM, 2 mL) for 2 h under the same conditions. For the study using LysoTracker, LysoTracker Green DND-26 (Molecular Probes, 2 μM in culture medium) was then added and the cells were incubated under these conditions for a further 10 min. For the study using MitoTracker, the cells were incubated with MitoTracker Green FM (Invitrogen, 0.25 μM in culture medium) for 10 min. For the study using ER-Tracker, the cells were incubated with ER-Tracker Green (Invitrogen, 0.2 μM in culture medium) for 20 min. For the study using SYTO-16, the cells were incubated with SYTO-16 (Invitrogen, 0.5 μM in culture medium) for 10 min. For all the cases, the cells were then rinsed with PBS and viewed with a Leica SP5 confocal laser-scanning microscope equipped with a 488 nm argon laser and a 633 nm helium−neon laser. All the Trackers were excited at 488 nm and monitored at 510−570 nm, while compound **11** was excited at 633 nm and monitored at 650−750 nm. Images were digitized and analyzed by Leica Application Suite Advanced Fluorescence Software. The subcellular localization of **11** was revealed by comparing the intracellular fluorescence images caused by the Trackers and this dye.

Flow Cytometric Studies. Approximately 6 × 10^5 HT29 cells in the medium (2 mL) were seeded on a 35 mm dish and incubated for 24 h at 37 °C under 5% CO_2. The cells were then treated with **11**, **12**, or **13** at their respective concentrations as indicated in Table 2 and incubated under the same conditions for 2 h. The cells were then rinsed thrice with PBS and refilled with the culture medium (2 mL) before being illuminated at ambient temperature using a halogen lamp light source as described above. After 24 h of incubation, the cells were rinsed with PBS and then harvested by 0.25% trypsin-EDTA (Invitrogen, 0.5 mL), followed by centrifugation at 2400 rpm for 3 min at room temperature. The pellet was then washed again by PBS and then subject to centrifugation. The cells were suspended in 1 mL of binding buffer (10 mM HEPES, 140 mM NaCl, 25 mM $CaCl_2$, pH = 7.4) containing annexin V-GFP (5 μL) and PI (2 μg mL^{-1}). After incubation in darkness for 15 min at room temperature, the signals of annexin V-GFP and PI were measured by a BD FACSCanto flow cytometer (Becton Dickinson) with 10^4 cells counted in each sample. Both annexin V-GFP and PI were excited by a 488 nm argon laser. The emitted fluorescence was monitored by at 500−560 nm for

annexin V-GFP and at >670 nm for PI. The data collected were analyzed by using WinMDI 2.9.

■ ASSOCIATED CONTENT

Supporting Information

Absorption and fluorescence spectra/data for **11** and **12** in DMF or DMEM, comparison of the rate of decay of DPBF sensitized by **11**, **12**, or ZnPc in DMF, results of subcellular localization studies, and ^{1}H and $^{13}C\{^{1}H\}$ NMR spectra of all the new compounds. This material is available free of charge via the Internet at http://pubs.acs.org.

■ AUTHOR INFORMATION

Corresponding Author

*For P.-C.L.: phone, (852) 3943 1326; fax, (852) 2603 5057; E-mail, pclo@cuhk.edu.hk. For D.K.P.N.: phone, (852) 3943 6375; fax, (852) 2603 5057; E-mail, dkpn@cuhk.edu.hk.

Notes

The authors declare no competing financial interest.

■ ACKNOWLEDGMENTS

We thank Sin-Lui Yeung for technical support in the in vitro studies. This work was supported by a grant from the Research Grant Council of the Hong Kong Special Administrative Region, China (project no. 402211).

■ ABBREVIATIONS USED

DBU, 1,8-diazabicyclo[5.4.0]undec-7-ene; DCFDA, 2′,7′-dichlorodihydrofluorescein diacetate; DMEM, Dulbecco's Modified Eagle's Medium; DMF, *N*,*N*-dimethylformamide; DPBF, 1,3-diphenylisobenzofuran; ESI, electrospray ionization; GFP, green fluorescent protein; PBS, phosphate buffered saline; PDT, photodynamic therapy; PI, propidium iodide; ROS, reactive oxygen species; SD, standard deviation; SEM, standard error of the mean; ZnPc, zinc(II) phthalocyanine; Φ_F, fluorescence quantum yield; Φ_Δ, singlet oxygen quantum yield; IC_{50}, dye concentration required to kill 50% of the cells

■ REFERENCES

(1) Dolmans, D. E. J. G. J.; Fukumura, D.; Jain, R. K. Photodynamic therapy for cancer. *Nature Rev. Cancer* **2003**, *3*, 380−387.

(2) Brown, S. B.; Brown, E. A.; Walker, I. The present and future role of photodynamic therapy in cancer treatment. *Lancet Oncol.* **2004**, *5*, 497−508.

(3) Celli, J. P.; Spring, B. Q.; Rizvi, I.; Evans, C. L.; Samkoe, K. S.; Verma, S.; Pogue, B. W.; Hasan, T. Imaging and photodynamic therapy: mechanisms, monitoring, and optimization. *Chem. Rev.* **2010**, *110*, 2795−2838.

(4) Robertson, C. A.; Evans, D. H.; Abrahamse, H. Photodynamic therapy (PDT): a short review on cellular mechanisms and cancer research applications for PDT. *J. Photochem. Photobiol., B* **2009**, *96*, 1−8.

(5) Zuluaga, M.-F.; Lange, N. Combination of photodynamic therapy with anti-cancer agents. *Curr. Med. Chem.* **2008**, *15*, 1655−1673.

(6) Nonaka, M.; Ikeda, H.; Inokuchi, T. Effects of combined photodynamic and chemotherapeutic treatment on lymphoma cells in vitro. *Cancer Lett.* **2002**, *184*, 171−178.

(7) Crescenzi, E.; Varriale, L.; Iovino, M.; Chiaviello, A.; Veneziani, B. M.; Palumbo, G. Photodynamic therapy with indocyanine green complements and enhances low-dose cisplatin cytotoxicity in MCF-7 breast cancer cells. *Mol. Cancer Ther.* **2004**, *3*, 537−544.

(8) He, P.; Ahn, J.-C.; Shin, J.-I.; Hwang, H.-J.; Kang, J.-W.; Lee, S.-J.; Chung, P.-S. Enhanced apoptotic effect of combined modality of 9-hydroxypheophorbide alpha-mediated photodynamic therapy and carboplatin on AMC-HN-3 human head and neck cancer cells. *Oncol. Rep.* **2009**, *21*, 329−334.

(9) Rizvi, I.; Celli, J. P.; Evans, C. L.; Abu-Yousif, A. O.; Muzikansky, A.; Pogue, B. W.; Finkelstein, D.; Hasan, T. Synergistic enhancement of carboplatin efficacy with photodynamic therapy in a three-dimensional model for micrometastatic ovarian cancer. *Cancer Res.* **2010**, *70*, 9319−9328.

(10) Snyder, J. W.; Greco, W. R.; Bellnier, D. A.; Vaughan, L.; Henderson, B. W. Photodynamic therapy: a means to enhanced drug delivery to tumors. *Cancer Res.* **2003**, *63*, 8126−8131.

(11) Kirveliene, V.; Grazeliene, G.; Dabkeviciene, D.; Micke, I.; Kirvelis, D.; Juodka, B.; Didziapetriene, J. Schedule-dependent interaction between doxorubicin and mTHPC-mediated photodynamic therapy in murine hepatoma in vitro and in vivo. *Cancer Chemother. Pharmacol.* **2006**, *57*, 65−72.

(12) Streckyte, G.; Didziapetriene, J.; Grazeliene, G.; Prasmickiene, G.; Sukeliene, D.; Kazlauskaite, N.; Characiejus, D.; Griciute, L.; Rotomskis, R. Effects of photodynamic therapy in combination with adriamycin. *Cancer Lett.* **1999**, *146*, 73−86.

(13) Lottner, C.; Bart, K.-C.; Bernhardt, G.; Brunner, H. Hematoporphyrin-derived soluble porphyrin−platinum conjugates with combined cytotoxic and phototoxic antitumor activity. *J. Med. Chem.* **2002**, *45*, 2064−2078.

(14) Lottner, C.; Knuechel, R.; Bernhardt, G.; Brunner, H. Combined chemotherapeutic and photodynamic treatment on human bladder cells by hematoporphyrin−platinum(II) conjugates. *Cancer Lett.* **2004**, *203*, 171−180.

(15) Lottner, C.; Knuechel, R.; Bernhardt, G.; Brunner, H. Distribution and subcellular localization of a water-soluble hematoporphyrin−platinum(II) complex in human bladder cancer cells. *Cancer Lett.* **2004**, *215*, 167−177.

(16) Mao, J.; Zhang, Y.; Zhu, J.; Zhang, C.; Guo, Z. Molecular combo of photodynamic therapeutic agent silicon(IV) phthalocyanine and anticancer drug cisplatin. *Chem. Commun.* **2009**, 908−910.

(17) Donzello, M. P.; Vittori, D.; Viola, E.; Manet, I.; Mannina, L.; Cellai, L.; Monti, S.; Ercolani, C. Tetra-2,3-pyrazinoporphyrazines with externally appended pyridine rings. 9. Novel heterobimetallic macrocycles and related hydrosoluble hexacations as potentially active photo/chemotherapeutic anticancer agents. *Inorg. Chem.* **2011**, *50*, 7391−7402.

(18) Manet, I.; Manoli, F.; Donzello, M. P.; Ercolani, C.; Vittori, D.; Cellai, L.; Masi, A.; Monti, S. Tetra-2,3-pyrazinoporphyrazines with externally appended pyridine rings. 10. A water-soluble bimetallic (Zn^{II}/Pt^{II}) porphyrazine hexacation as potential plurimodal agent for cancer therapy: exploring the behavior as ligand of telomeric DNA G-quadruplex structures. *Inorg. Chem.* **2011**, *50*, 7403−7411.

(19) Králová, J.; Kejík, Z.; Bříza, T.; Poučková, P.; Král, A.; Martásek, P.; Král, V. Porphyrin−cyclodextrin conjugates as a nanosystem for versatile drug delivery and multimodal cancer therapy. *J. Med. Chem.* **2010**, *53*, 128−138.

(20) Kim, J.; Yoon, H.-J.; Kim, S.; Wang, K.; Ishii, T.; Kim, Y.-R.; Jang, W.-D. Polymer−metal complex micelles for the combination of sustained drug releasing and photodynamic therapy. *J. Mater. Chem.* **2009**, *19*, 4627−4631.

(21) Peng, C.-L.; Lai, P.-S.; Lin, F.-H.; Wu, S. Y.-H.; Shieh, M.-J. Dual chemotherapy and photodynamic therapy in an HT-29 human colon cancer xenograft model using SN-38-loaded chlorin-core star block copolymer micelles. *Biomaterials* **2009**, *30*, 3614−3625.

(22) Shieh, M.-J.; Hsu, C.-Y.; Huang, L.-Y.; Chen, H.-Y.; Huang, F.-H.; Lai, P.-S. Reversal of doxorubicin-resistance by multifunctional nanoparticles in MCF-7/ADR cells. *J. Controlled Release* **2011**, *152*, 418−425.

(23) Jiang, X.-J.; Yeung, S.-L.; Lo, P.-C.; Fong, W.-P.; Ng, D. K. P. Phthalocyanine−polyamine conjugates as highly efficient photosensitizers for photodynamic therapy. *J. Med. Chem.* **2011**, *54*, 320−330 and references cited therein..

(24) Lau, J. T. F.; Lo, P.-C.; Fong, W.-P.; Ng, D. K. P. Preparation and photodynamic activities of silicon(IV) phthalocyanines substituted

with permethylated β-cyclodextrins. *Chem.—Eur. J.* **2011**, *17*, 7569−7577.
(25) Lau, J. T. F.; Lo, P.-C.; Tsang, Y.-M.; Fong, W.-P.; Ng, D. K. P. Unsymmetrical β-cyclodextrin-conjugated silicon(IV) phthalocyanines as highly potent photosensitisers for photodynamic therapy. *Chem. Commun.* **2011**, *47*, 9657−9659.
(26) He, H.; Lo, P.-C; Yeung, S.-L.; Fong, W.-P.; Ng, D. K. P. Preparation of unsymmetrical distyryl BODIPY derivatives and effects of the styryl substituents on their in vitro photodynamic properties. *Chem. Commun.* **2011**, *47*, 4748−4750.
(27) He, H.; Lo, P.-C; Yeung, S.-L.; Fong, W.-P.; Ng, D. K. P. Synthesis and in vitro photodynamic activities of pegylated distyryl boron dipyrromethene derivatives. *J. Med. Chem.* **2011**, *54*, 3097−3102.
(28) Wong, E.; Giandomenico, C. M. Current status of platinum-based antitumor drugs. *Chem. Rev.* **1999**, *99*, 2451−2466.
(29) Kelland, L. The resurgence of platinum-based cancer chemotherapy. *Nature Rev. Cancer* **2007**, *7*, 573−584.
(30) Liu, J.-Y.; Jiang, X.-J.; Fong, W.-P.; Ng, D. K. P. Highly photocytotoxic 1,4-dipegylated zinc(II) phthalocyanines. Effects of the chain length on the in vitro photodynamic activities. *Org. Biomol. Chem.* **2008**, *6*, 4560−4566.
(31) Liu, J.-Y.; Lo, P.-C.; Fong, W.-P.; Ng, D. K. P. Effects of the number and position of the substituents on the in vitro photodynamic activities of glucosylated zinc(II) phthalocyanines. *Org. Biomol. Chem.* **2009**, *7*, 1583−1591.
(32) Liu, J.-Y.; Lo, P.-C.; Jiang, X.-J.; Fong, W.-P.; Ng, D. K. P. Synthesis and in vitro photodynamic activities of di-α-substituted zinc(II) phthalocyanine derivatives. *Dalton Trans.* **2009**, 4129−4135.
(33) Stein, A.; Arnold, D. Oxaliplatin: a review of approved uses. *Expert Opin. Pharmacother.* **2012**, *13*, 125−137.
(34) Loiseau, F. A.; Hill, A. M.; Hii, K. K. Preparation of macrocyclon analogues: calix[8]arenes with extended polyethylene glycol chains. *Tetrahedron* **2007**, *63*, 9947−9959.
(35) Wyrick, S. D.; Chaney, S. G. Tritiated platinum antitumor agents containing the *trans*-(D,L)-1,2-diaminocyclohexane carrier ligand. *J. Labelled Compd. Radiopharm.* **1988**, *25*, 349−357.
(36) Erdem, S. S.; Nesterova, I. V.; Soper, S. A.; Hammer, R. P. Solid-phase synthesis of asymmetrically substituted "AB_3-type" phthalocyanines. *J. Org. Chem.* **2008**, *73*, 5003−5007.
(37) Scalise, I.; Durantini, E. N. Synthesis, properties, and photodynamic inactivation of *Escherichia coli* using a cationic and a noncharged Zn(II) pyridyloxyphthalocyanine derivatives. *Bioorg. Med. Chem.* **2005**, *13*, 3037−3045.
(38) Maree, M. D.; Kuznetsova, N.; Nyokong, T. Silicon octaphenoxyphthalocyanines: photostability and singlet oxygen quantum yields. *J. Photochem. Photobiol., A* **2001**, *140*, 117−125.
(39) Balin-Gauthier, D.; Delord, J.-P.; Rochaix, P.; Mallard, V.; Thomas, F.; Hennebelle, I.; Bugat, R.; Canal, P.; Allal, C. In vivo and in vitro antitumor activity of oxaliplatin in combination with cetuximab in human colorectal tumor cell lines expressing different level of EGFR. *Cancer Chemother. Pharmol.* **2006**, *57*, 709−718.
(40) Shen, H. M.; Shi, C. Y.; Shen, Y.; Ong, C. N. Detection of elevated reactive oxygen species level in cultured rat hepatocytes treated with aflatoxin B-1. *Free Radical Biol. Med.* **1996**, *21*, 139−146.
(41) Vermes, I.; Haanen, C.; Steffens-Nakken, H.; Reutelingsperger, C. A novel assay for apoptosis. Flow cytometric detection of phosphatidylserine expression on early apoptotic cells using fluorescein labelled annexin V. *J. Immunol. Methods* **1995**, *184*, 39−51.
(42) Eaton, D. F. Reference materials for fluorescence measurements. *Pure Appl. Chem.* **1988**, *60*, 1107−1114.
(43) Tada, H.; Shiho, O.; Kuroshima, K.; Koyama, M.; Tsukamoto, K. An improved colorimetric assay for interleukin-2. *J. Immunol. Methods* **1986**, *93*, 157−165.